Supplementary Material

Synergistic Charge Storage Enhancement in Supercapacitors via $Ti_3C_2T_x$ MXene and $CoMoO_4$ Nanoparticles

Christine Young *, An-Yi Wu and Ri-Yu Li

Functional Nanoporous Materials Laboratory, Department of Chemical and Materials Engineering, National Yunlin University of Science and Technology, Yunlin 640, Taiwan

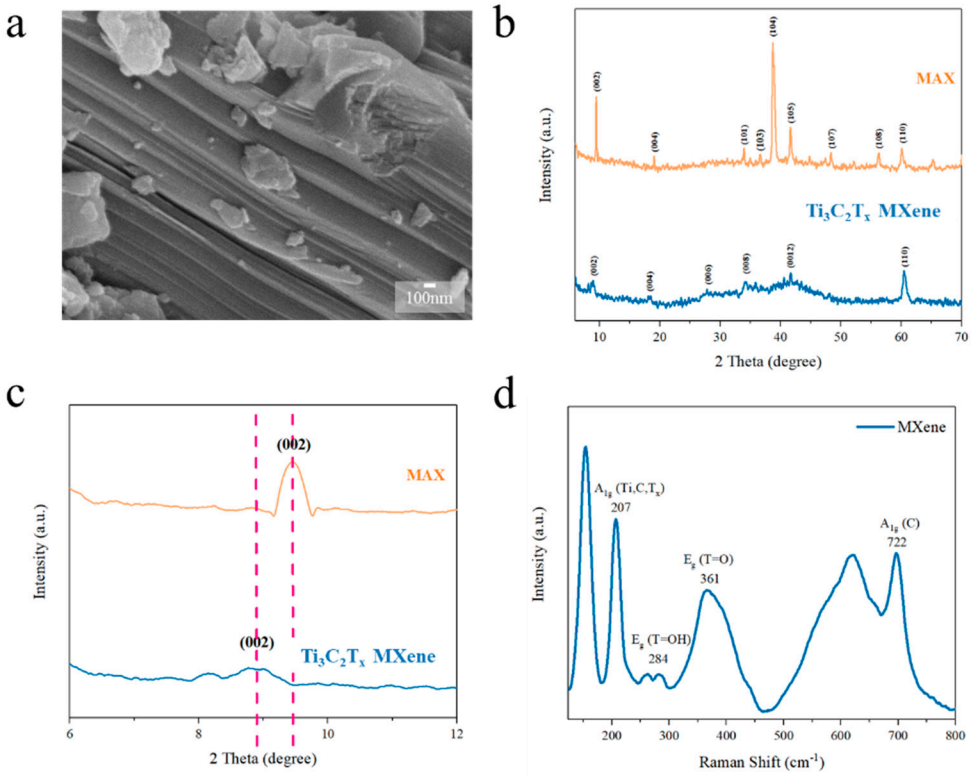

Figure S1. (a) SEM image of MAX. (b,c) XRD patterns of MAX and $Ti_3C_2T_x$ MXene. (d) Raman spectrum of $Ti_3C_2T_x$ MXene.

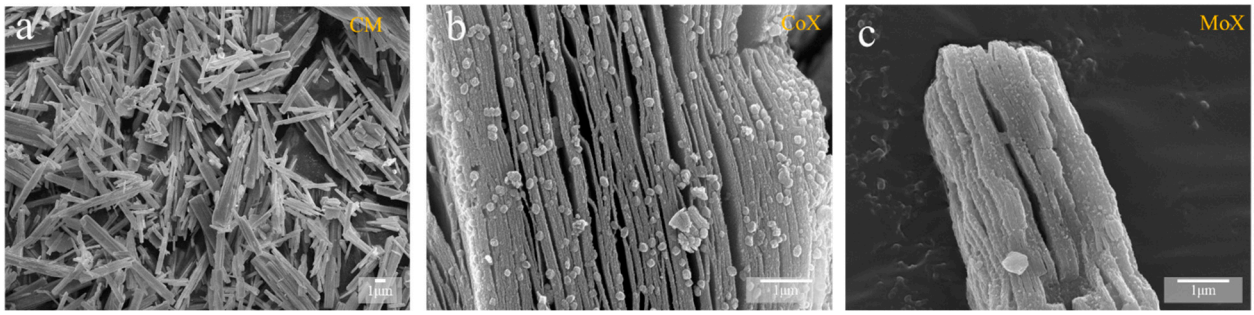

Figure S2. SEM images of (a) CM, (b) CoX, and (c) MoX.

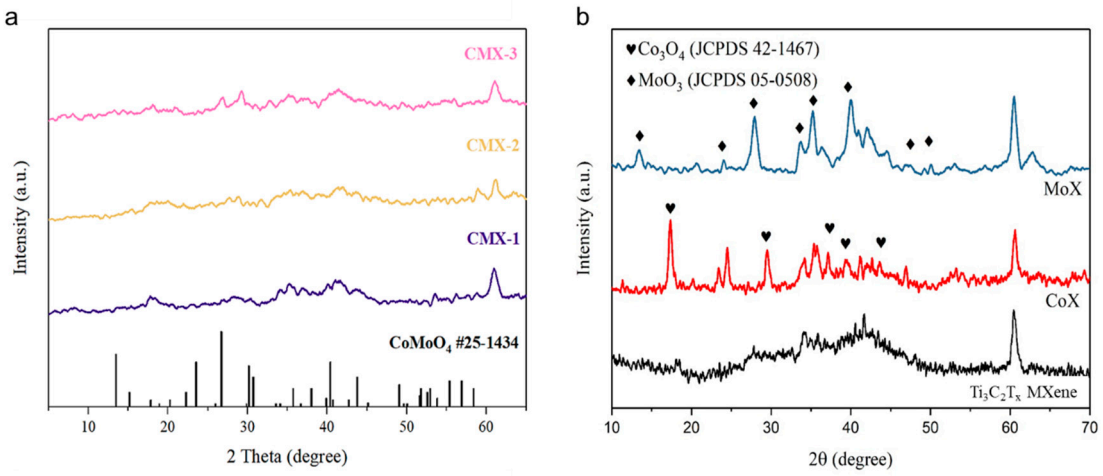

Figure S3. (a) XRD patterns of CMX-1, CMX-2, and CMX-3. (b) XRD patterns of $Ti_3C_2T_x$ MXene, CoX, and MoX.

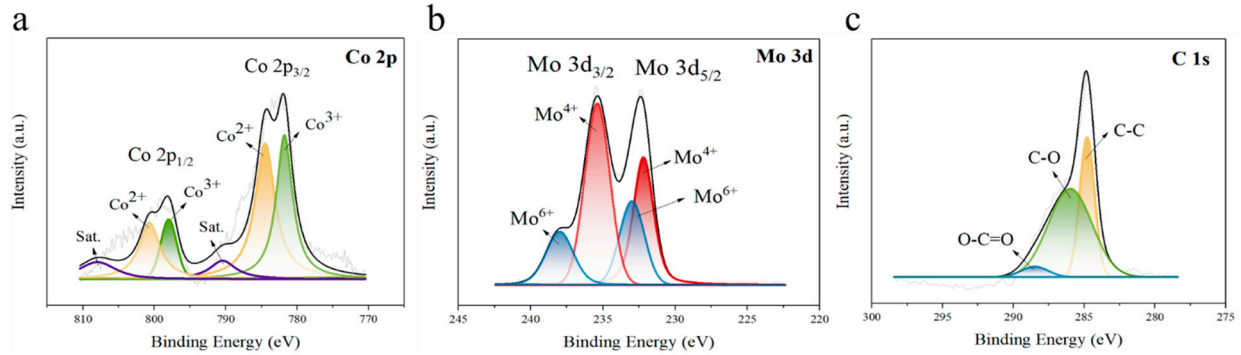

Figure S4. High resolution XPS spectra showing the (a) Co 2p, (b) Mo 3d and (c) C 1s for CMX-1.

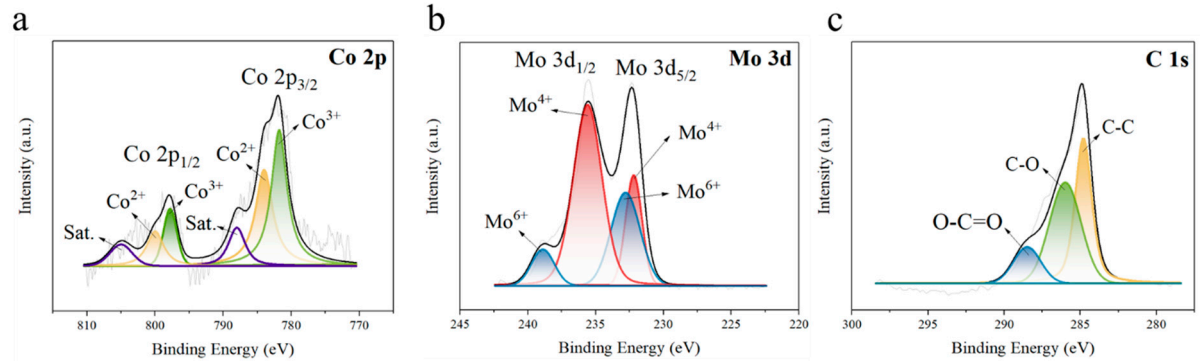

Figure S5. High resolution XPS spectra showing the (a) Co 2p, (b) Mo 3d and (c) C 1s for CMX-3.

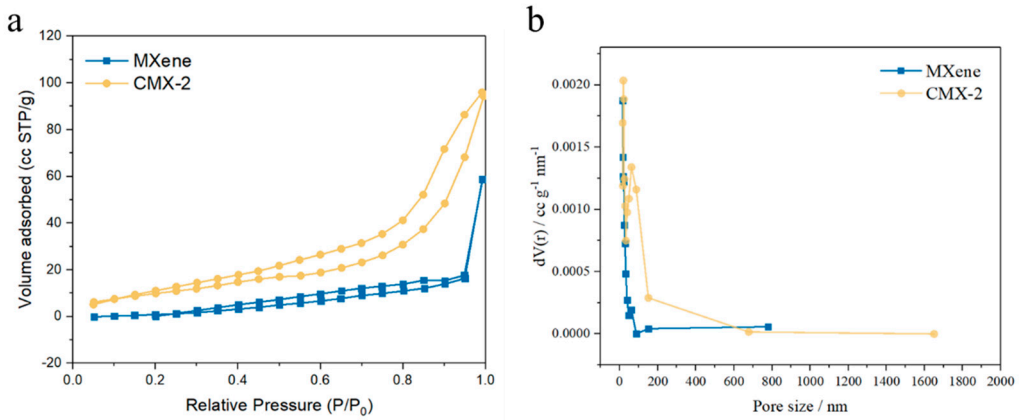

Figure S6. (a) Nitrogen adsorption-desorption isotherms for $Ti_3C_2T_x$ MXene and CMX-2. (b) Pore size distribution of $Ti_3C_2T_x$ MXene and CMX-2 determined using BJH method.

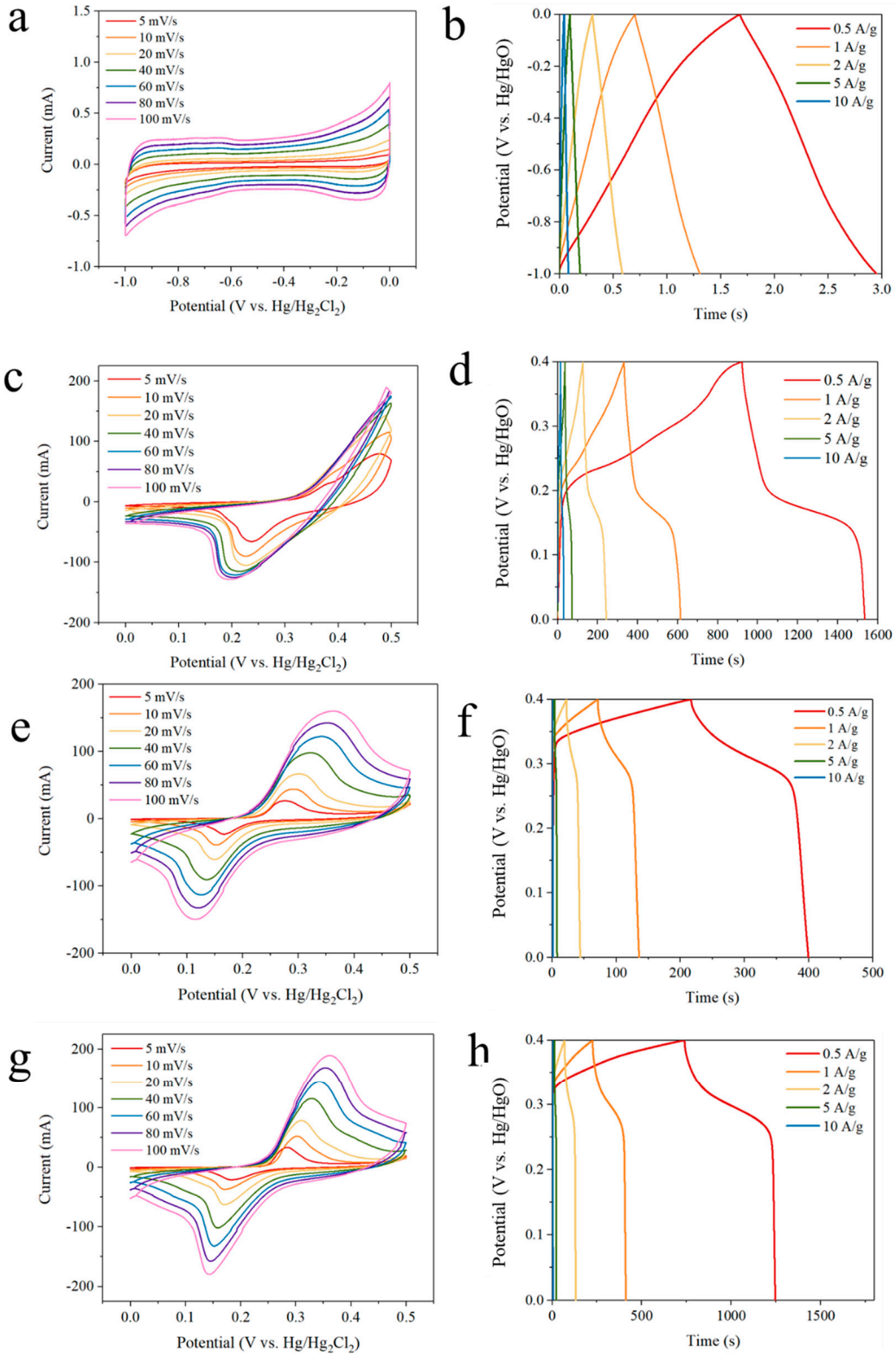

Figure S7. CV curves and GCD curves of (a,b) $Ti_3C_2T_x$ MXene, (c,d) CM, (e,f) CoX, and (g,h) MoX.

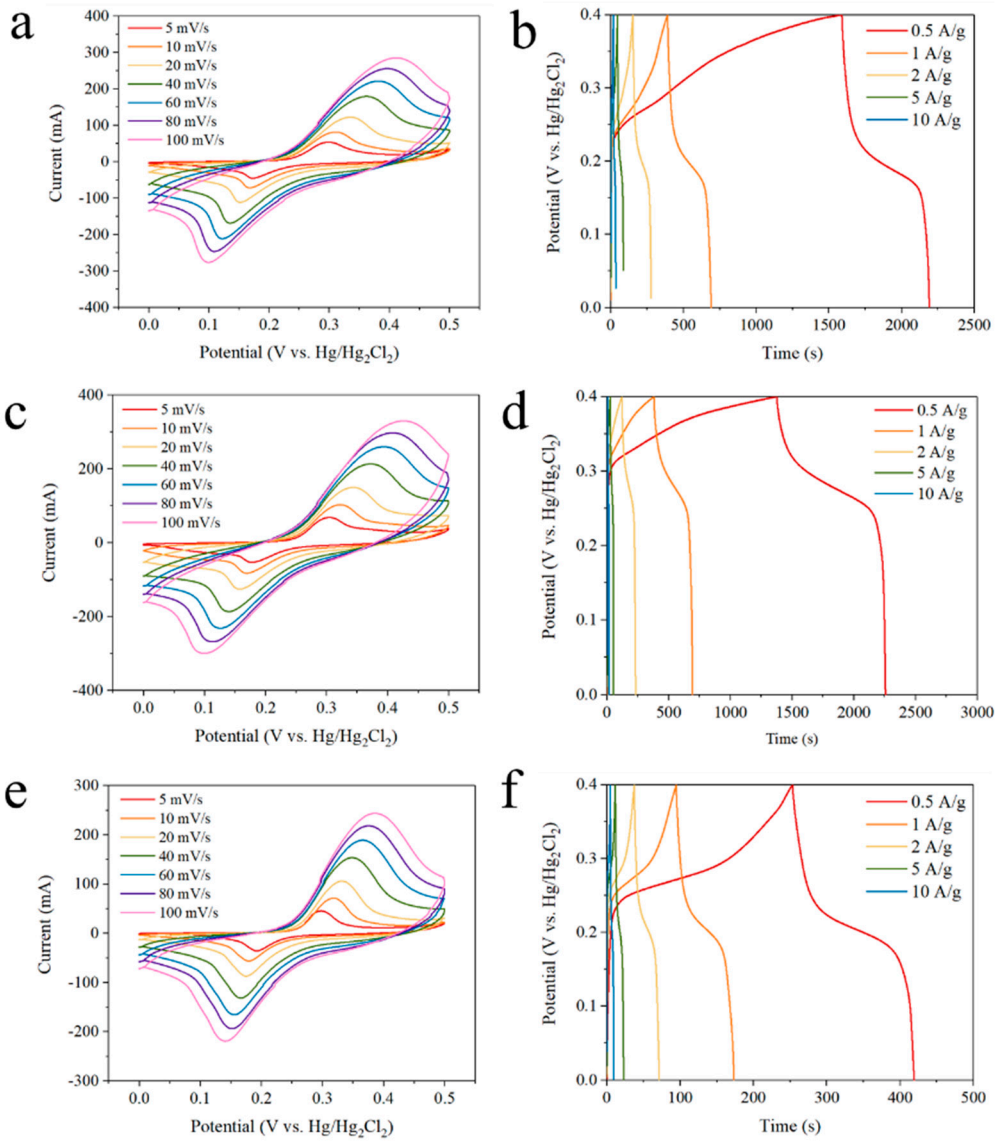

Figure S8. CV curves and GCD curves of (a,b) CMX-1, (c,d) CMX-2, and (e,f) CMX-3.

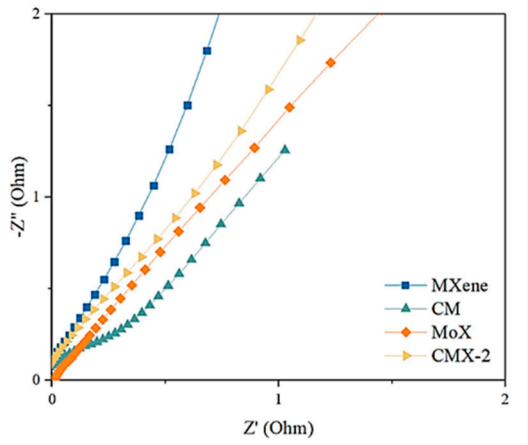

Figure S9. The Nyquist plot of $Ti_3C_2T_x$ MXene, CM, MoX, and CMX-2.

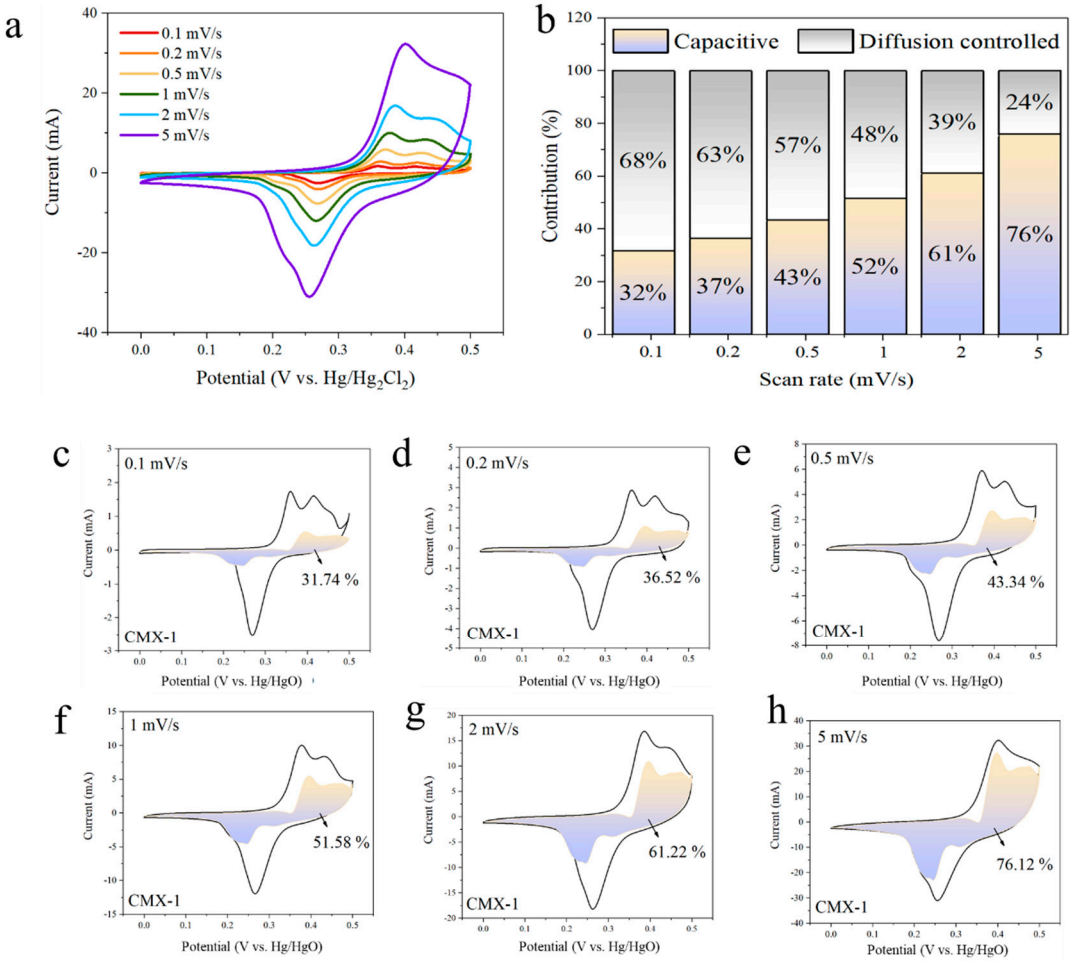

Figure S10. (a) CV curves of CMX-1 at the scan rates of 0.1, 0.2, 0.5, 1, 2, 5 mV s^{-1}. (b) Capacitive and diffusion controlled contribution at various scan rates for CMX-1. (c–h) CV curves showing the capacitive and diffusion-controlled contributions at the scan rates ranging from 0.1 to 5 mV s^{-1}.

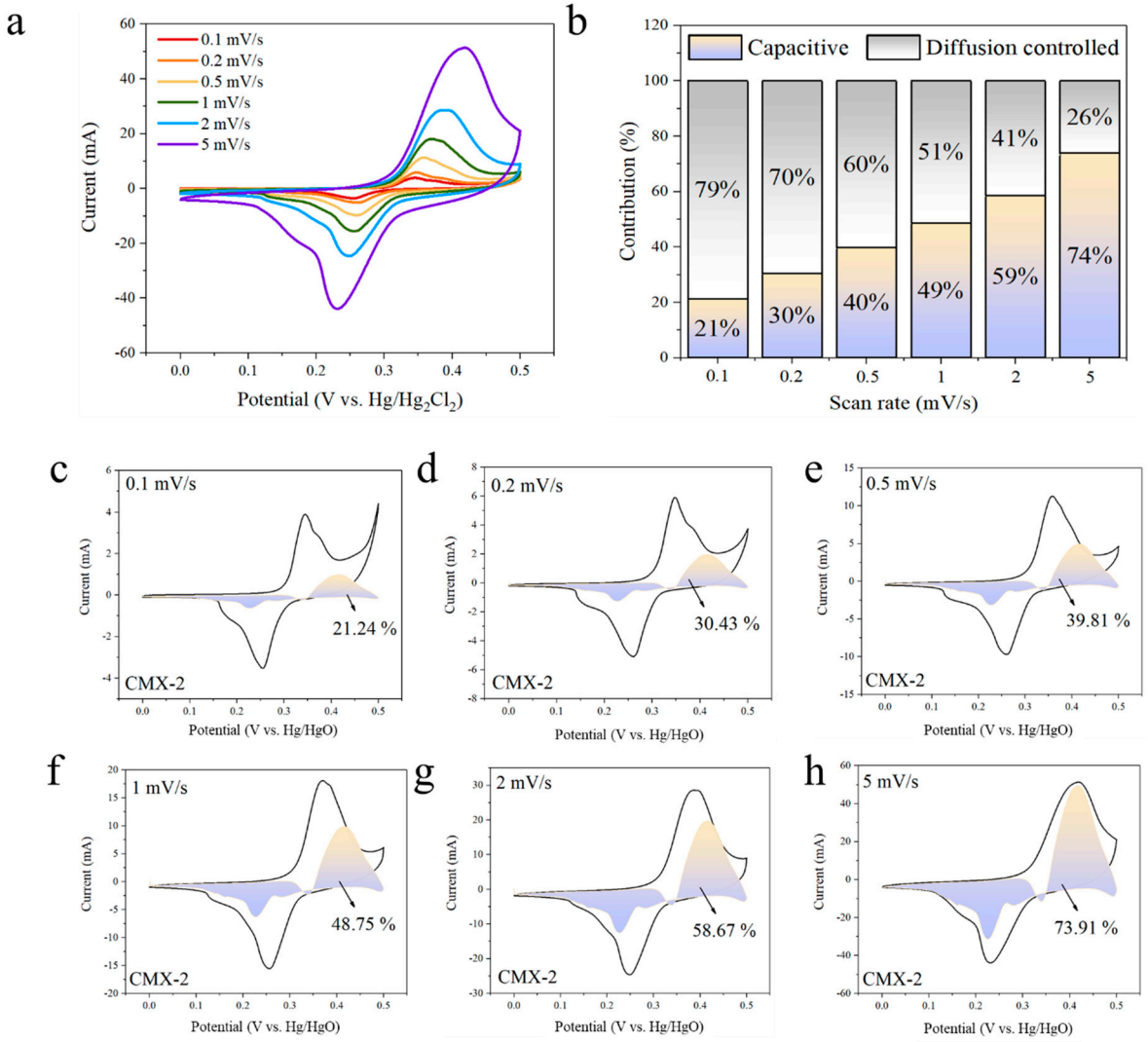

Figure S11. (a) CV curves of CMX-2 at the scan rates of 0.1, 0.2, 0.5, 1, 2, 5 mV s^{-1}. (b) Capacitive and diffusion controlled contribution at various scan rates for CMX-2. (c–h) CV curves showing the capacitive and diffusion-controlled contributions at the scan rates ranging from 0.1 to 5 mV s^{-1}.

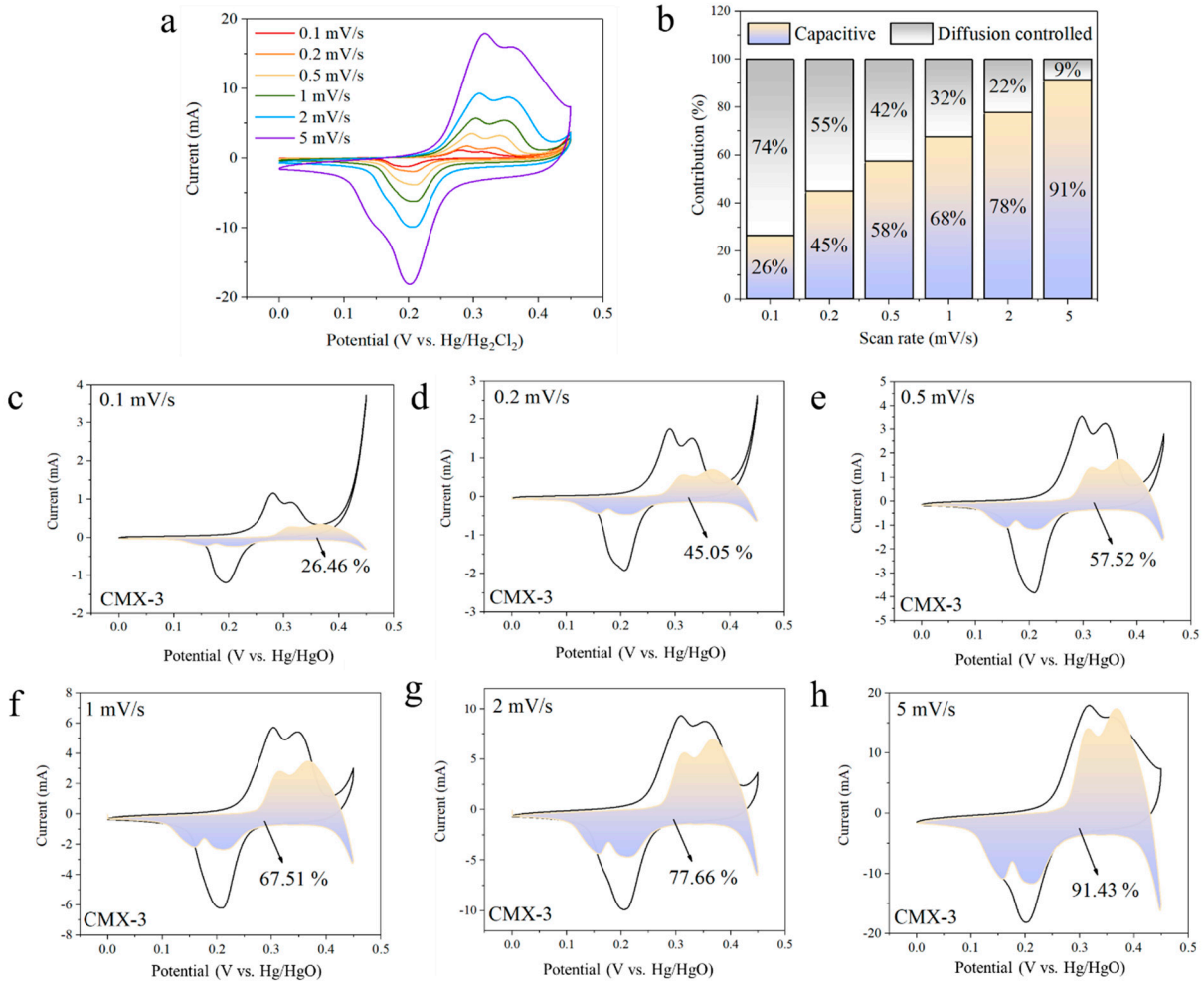

Figure S12. (a) CV curves of CMX-3 at the scan rates of 0.1, 0.2, 0.5, 1, 2, 5 mV s^{-1}. (b) Capacitive and diffusion controlled contribution at various scan rates for CMX-3. (c–h) CV curves showing the capacitive and diffusion-controlled contributions at the scan rates ranging from 0.1 to 5 mV s^{-1}.

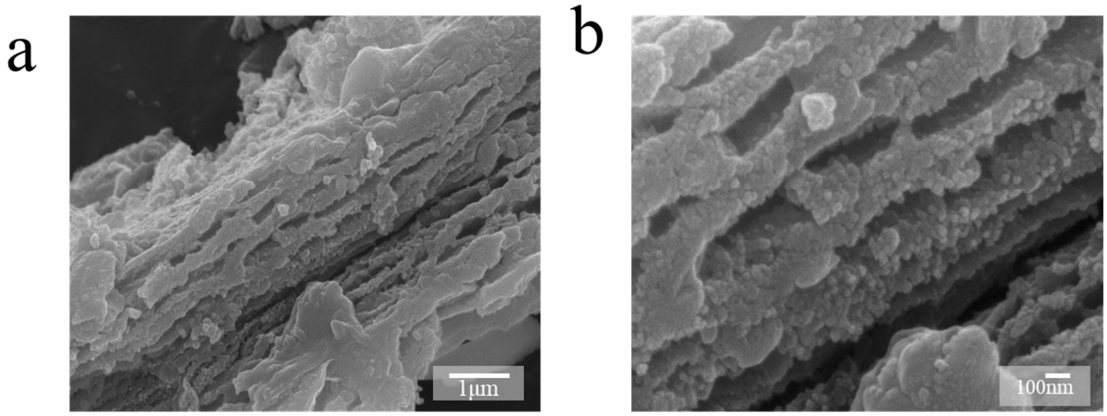

Figure S13. SEM images of CMX-2 after stability test.

Table S1. The element component ratio of CMX-1, CMX-2, and CMX-3.

Sample	C (at%)	O (at%)	Co (at%)	Mo (at%)	Ti (at%)	Al (at%)
CMX-1	50.2	31.6	10.0	6.6	1.6	<0.1
CMX-2	60.6	28.0	5.1	4.5	1.8	<0.1
CMX-3	58.6	27.4	4.9	6.5	2.6	<0.1